Refining gravity anomaly data of coastal areas by combining XGM2019e-2159 and SRTM/GEBCO_2024 residual terrain model with forward modeling method

Yixiang Liu[1], Jinyun Guo[1*], Bin Guan[2], Shaofeng Bian[3], Heping Sun[4], Xin Liu[1]

[1]*College of Geodesy and Geomatics, Shandong University of Science and Technology, Qingdao 266590, China；*

[2]*State Key Laboratory of Geoinformation Engineering, Xi'an Research Institute of Surveying and Mapping, Xi'an 710054, China；*

[3]*Key Laboratory of Geological Survey and Evaluation of Ministry of Education, China University of Geosciences, Wuhan 430074，China；*

[4]*State Key Laboratory of Precision Geodesy，Innovation Academy for Precision Measurement Science and Technology, Chinese Academy of Sciences, Wuhan 430077, China*

** Corresponding author: Jinyun Guo (jinyunguo1@126.com)*

Abstract. As one of the Earth's fundamental physical fields, the gravity field model's accuracy is considerably constrained in areas with sparse coverage or data gaps. In coastal areas, satellite altimetry data are affected by land contamination and errors from tidal models, while shipborne gravity measurements fail to obtain valid gravity data in nearshore regions. Therefore, gravity field models' accuracy in coastal areas is relatively lower. Additionally, due to the truncation of global gravity field models at specific degrees, truncation errors prevent the acquisition of high-precision gravity anomaly (GA) information. To address this issue, a gravity forward modeling-based refinement method using the residual terrain model (RTM) is proposed for coastal regions. In this study, a mass center offset correction (MCOC) is introduced as the main innovation to mitigate prism position shift errors induced by the rock-equivalent topography (RET) method. Specifically, a high-resolution detailed topography model of the study area, referred to as the SRTM–GEBCO model, was first constructed by merging the land digital elevation model SRTM V4.1 with the ocean bathymetric model GEBCO_2024. Based on this model, the reference topography was then derived using a spatial filtering approach based on the moving average method. The RTM is then discretized into regular grid prisms, and the GA generated by the RTM at target points is computed in the spatial domain using the prism integration method to refine the XGM2019e-2159 gravity anomaly (XGM-GA) model. For computation points located in coastal areas, the RET method is adopted to avoid distinguishing between the densities of land and ocean prisms during forward modeling, and the MCOC is further applied to correct the resulting positional bias. To validate the feasibility of this method, this study focuses on a selected region along the U.S. West Coast (125°W–122°W, 39°N–42°N) and refines the XGM-GA model. The experimental results are validated using NGS99 measured GA data. The results indicate that, after RTM correction, the root mean square difference between the modeled and measured GA decreases from 14.58mGal to 8.25mGal overall and from 14.98mGal to 7.97mGal in coastal areas. Furthermore, power spectral density analysis of the XGM-GA

model before and after RTM correction reveals a significant enhancement in short-wavelength energy in the corrected model. The results demonstrate that gravity forward modeling based on the RTM is effective in compensating for the truncation errors of the XGM-GA model, thereby improving its accuracy.

1. Introduction

Global gravity field models with high spatial resolution and accuracy have significant scientific and practical value in fields such as geodesy, glaciology, hydrology, solid Earth geophysics, natural disaster monitoring, and resource exploration (Han et al., 2015; Dubey and Roy, 2023; Liang et al., 2023). With the advancement of satellite altimetry technology and the improvement in the quality of shipborne data, both satellite altimetry data and shipborne measurements have become the primary sources for determining regional marine gravity fields (Andersen et al., 2010; Li et al., 2024; Zhou et al., 2025). However, in coastal areas, satellite altimetry data are influenced by land interference and various errors, such as those in tidal models (Hwang, 1997; Guo et al., 2010; Claessens, 2011). Furthermore, due to the distance of 5-30 km between the shipborne gravity survey lines and the coastline on the landward side, shipborne gravity measurements in this range are unable to obtain valid data, resulting in a data gap in the coastal region (Ke et al., 2019). The widely used global gravity field models, including XGM2019e-2159 (Zingerle et al., 2020) and EGM2008 (Pavlis et al., 2012), are represented using spherical harmonic functions. These models can be used to calculate the gravity anomaly (GA) at any point on the Earth's surface and in outer space. However, due to the truncation of the spherical harmonic model at degree 2159, it cannot reflect high-frequency GA information beyond this degree (Gruber, 2009). Since the high-frequency signals of gravity field models are primarily provided by the Earth's topography, these errors have a smaller impact in flat regions, but tend to have a larger effect in rugged mountainous areas and the coastal regions with complex terrain (Hirt, 2010). Therefore, effectively integrating topographic information into existing high-degree gravity field models is a primary method for refining regional gravity field data.

The use of detailed topography data to refine gravity field models has gained extensive research and attention in recent decades. The results of using residual terrain model (RTM) methods to calculate topographic gravity effects in rugged mountainous areas based on high-resolution digital elevation models show that RTM methods can effectively compensate for truncation errors in GA models (Forsberg and Tscherning, 1981; Liu et al., 2025). If bathymetric data are incorporated and differences between water and crustal densities within the integration region are taken into account, the geoid model refined by RTM forward modeling with detailed topographic data can be significantly improved in accuracy (Li et al., 2024). Validation with ground-measured data showed that the high-frequency components of vertical deflections derived from RTM gravity forward modeling can effectively compensate for the truncation errors of the EGM2008 and XGM2019e-2159 vertical deflection models (Hirt et al., 2010b; Liu et al., 2025).

Gravity forward modeling based on the RTM can be conducted in either the frequency domain (Tenzer, 2005; Yang et al., 2019; Ince et al., 2020; Wu et al., 2023) or the spatial domain (Smith, 2000; Wild-Pfeiffer, 2008; Tsoulis et al., 2009). Although the frequency-domain approach offers higher computational efficiency, its accuracy is generally lower than that of spatial domain methods (Parker, 1995). Research on gravity forward modeling in the spatial domain mainly aims to improve the accuracy of forward results. Therefore, this study adopts the spatial-domain approach to refine the modeled GA in coastal areas. The traditional RTM method assumes a uniform density for the residual terrain within the integration region. However, if the region includes other types of landforms such as lakes, oceans, or ice sheets, this assumption of uniform prism density can lead to significant errors. In such cases, the traditional RTM method struggles to obtain a reasonable residual terrain model, necessitating improvements to meet the application requirements in complex topographic regions. To address this, Hirt (2013) improved the traditional method by merging detailed topography and bathymetric data and adopting the rock-equivalent topography (RET) method. This approach allows for a single constant prism density within the integration region, eliminating the need to distinguish between land and ocean prisms (Kuhn and Hirt, 2016). Based on gravity forward modeling theory, topographic information can be transformed into corresponding gravity field signals. In the process of constructing the RTM from detailed and reference topography, the reference model acts as a high-pass filter, and the resulting RTM retains the high-frequency components of the topographic data (Hirt, 2010). The reference topographic model can be obtained either from the spherical harmonic expansion of the detailed topography or by applying a smoothing filter to the detailed model (Lin et al., 2023). When the reference topography is derived through spherical harmonic expansion of the detailed terrain using the same degree as that of the refined GA model, the GA computed from the RTM can effectively extend its high-frequency components. Generally, in areas with rugged and complex terrain, gravity field model lacks sufficient high-frequency GA signals, resulting in lower model accuracy.

This study aims to improve the accuracy of the XGM2019e-2159 gravity anomaly (XGM-GA) model in coastal regions and to compensate for truncation errors. The 3″×3″ SRTM V4.1 terrestrial digital elevation model data are first integrated with the 15″×15″ GEBCO_2024 marine bathymetry data to construct a combined SRTM–GEBCO dataset. Based on this dataset, a reference topography model is constructed using a spatial filtering approach based on the moving average (MA) method, from which the RTM is derived. Subsequently, the high-frequency gravity anomalies of the RTM within the study area are computed in the spatial domain, and are used to refine the XGM2019e-2159 gravity anomaly model.

2. Study area and data

2.1 Study area

The study area (125°W–122°W, 39°N–42°N) is located on the west coast of the United States. Since the calculation of RTM-GA at a given point requires elevation data from a surrounding region, the terrain and bathymetric data coverage is

extended to 126°W–121°W, 38°N–43°N. The topography of the study area and its surroundings is shown in Fig. 1. The study area borders the Pacific Ocean to the west and includes the Central Valley, the Sierra Nevada, and the Cascade Range. The highest elevation point is Mount Shasta, located in the southern Cascade Range, with an elevation of 4316 meters. The complex topographic environment of the study area implies that the GA information provided by global gravity field models lacks significant high-frequency GA signals.

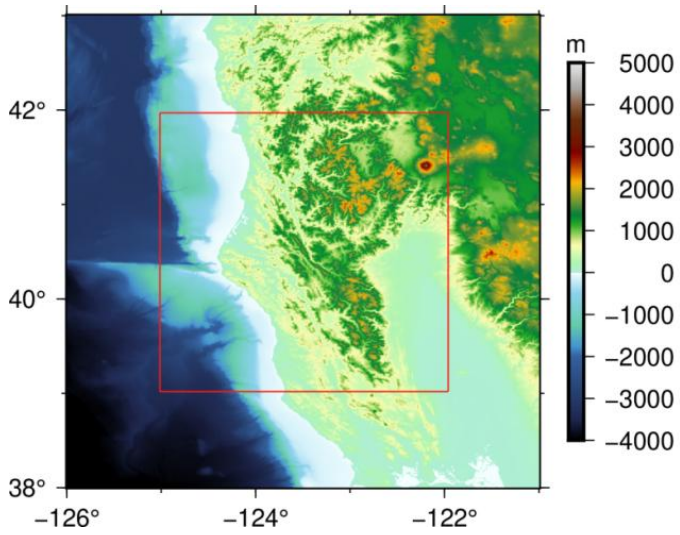

Figure 1: Study area boundary (red box) and surrounding topography.

2.2 Global Gravity Field Model

XGM2019e is a global gravity field model developed by integrating terrestrial gravity observations with satellite-derived data. In the high-frequency spectral range, noise contributions from both data sources must be carefully addressed. In particular, coastal regions and areas with sparse or missing ground data are more prone to noise-induced distortions in the model signal. To suppress such effects, a weighted smoothing transition strategy is applied. Nevertheless, even after these procedures, the signal-to-noise ratio (SNR) at higher harmonic degrees remains relatively low, leading to attenuation of true signals and thereby constraining the practical use of high-degree gravity field models (Zingerle et al., 2020). Consequently, adopting a limited set of spherical harmonic coefficients instead of all high-degree terms provides a better trade-off between spatial resolution and SNR. Accordingly, the XGM2019e-2159 model, expanded up to degree 2159 and corresponding to a spatial resolution of 5′×5′, is adopted in this study. The model is constructed based on several datasets, including the combined satellite-only gravity field model GOCO06s, ground GA data provided by the National Geospatial-Intelligence Agency, and DTU13 marine GA derived from satellite radar altimetry. The GA model derived from XGM2019e-2159 can be computed via the International Centre for Global Earth Models (ICGEM) website (http://icgem.gfz-potsdam.de/calcgrid).

2.3 Digital Elevation and Bathymetric Models

This study uses the high-resolution SRTM V4.1 dataset as the digital elevation model, which was acquired from the Shuttle Radar Topography Mission (SRTM) (https://srtm.csi.cgiar.org). This mission was a collaboration between the National

Imagery and Mapping Agency and the National Aeronautics and Space Administration. The elevation data of SRTM V4.1 are referenced to the EGM96 geoid, with a spatial resolution of 3″ × 3″. SRTMV4.1 employs a new interpolation algorithm and supplementary DEM data to fill data voids present in SRTM3, resulting in significantly improved elevation accuracy compared to SRTM3 (Reuter et al., 2007).

The bathymetric data in this study are sourced from GEBCO (General Bathymetric Chart of the Oceans), a project based on the Global Earth System Project. The dataset encompasses global DEM data ranging from grid scale to basin scale, integrating multiple bathymetric data sources, including shipborne echo sounding, satellite altimetry data, and other high-resolution bathymetric measurements. The GEBCO_2024 dataset used in this study was released in July 2024 (https://www.gebco.net). It provides globally comprehensive elevation data on a 15″×15″ geographic grid (Tozer et al., 2019).

2.4 Measured GA Data

This study uses the measured gravity data NGS99, published by the National Geodetic Survey (NGS), as the reference dataset (https://www.ncei.noaa.gov/products/gravity-data). The NGS99 dataset includes 1,633,499 discrete gravity measurement points. The NGS99 gravity data cover not only the inland regions of the United States but also extend to its coastal areas. Figure 2 illustrates the distribution of NGS99 measured GA values and measurement locations within the study area, comprising 10,797 oceanic points and 3,247 land-based points.

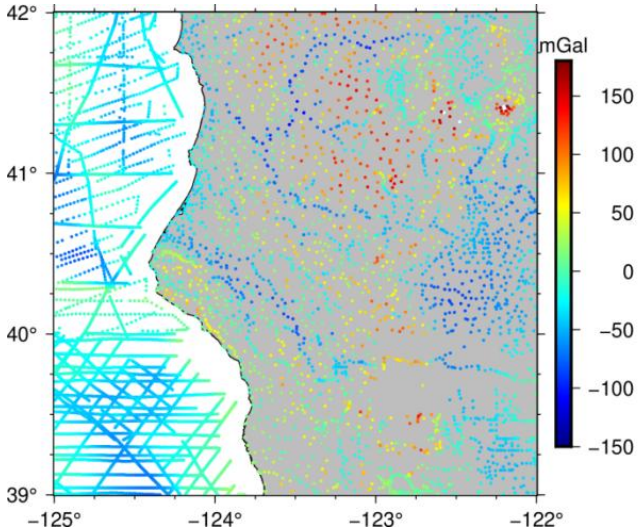

Figure 2: Distribution of NGS99 measured GA points in the study area.

3. Methodology

3.1 Construction of the RTM

According to the definition, RTM represents the difference between the detailed and reference topography. Due to the resolution mismatch between the 3″×3″ topographic data SRTM V4.1 on land and the 15″×15″ bathymetric data

GEBCO_2024 in the ocean, and the fact that SRTM V4.1 data is only available on land, the two models must be merged before constructing the residual terrain model. First, bicubic interpolation is applied to interpolate GEBCO_2024 to a 3″×3″ grid, matching the resolution of SRTM V4.1. Then, the terrestrial data in the study area from GEBCO_2024 is removed, and the terrestrial data from SRTM V4.1 is incorporated into GEBCO_2024. This process yields the detailed topography model SRTM-GEBCO required for this study.

The reference topography model is obtained by applying a spatial filtering approach based on the moving average to the SRTM-GEBCO data. The core idea of this method is to replace the value of a target point with the average of all points within a certain neighborhood around it. In essence, it acts as a low-pass filter, removing high-frequency topographic details while retaining low-frequency large-scale topographic variations. To maintain consistency with the spatial resolution of the XGM2019e-2159 gravity field model, we set the resolution of the filtered reference terrain model to 5′×5′ as well.

The elevation of the aforementioned detailed topography model SRTM-GEBCO is denoted as H^{DET} and the elevation of the reference topography model obtained by spatial filtering is denoted as H^{REF}. Then, the elevation of the RTM can be expressed as:

$$\Delta H^{\mathrm{RTM}} = H^{DET} - H^{\mathrm{REF}}. \tag{1}$$

The schematic diagram of the RTM for land and marine areas is shown in Fig. 3, where the RTM for the marine area is obtained using the RET method.

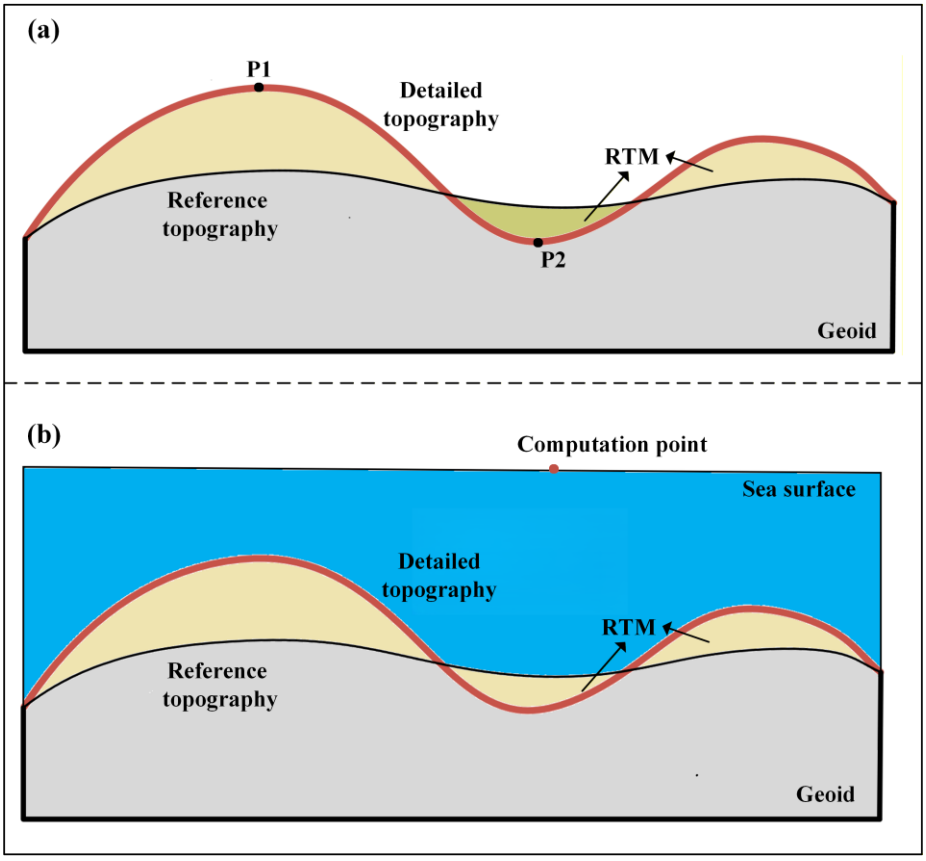

Figure 3: Schematic diagrams of the RTM over land (a) and over the marine area (b).

The RTM of the study area is obtained using the above method, as shown in Fig. 4. In the marine regions, the RTM is constructed using the RET method. A comparison between Figs. 1 and 4 reveals that the residual terrain elevation exhibits alternating positive and negative values in areas with significant terrain undulation, with a maximum reaching over 800 m and a minimum below -700 m. In contrast, in oceanic regions and relatively flat plains or valleys, the variation in residual terrain elevation is also smaller.

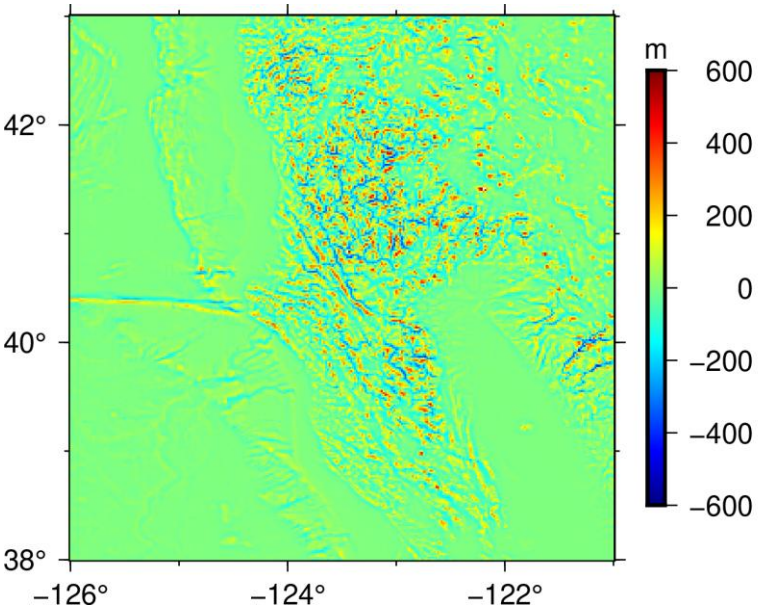

Figure 4 : RTM of the study area with RET applied in the marine area.

3.2 Method for Calculating RTM-GA

This study refines the Earth's GA model in coastal areas using a spatial domain approach. First, the residual terrain is divided into discrete prism-shaped units, and the gravitational influence of each unit on the observation point is calculated. Then, the cumulative effect of all these units provides the gravitational contribution from the residual terrain at the location of interest. Due to the oscillation of RTM elevations between negative and positive values within a certain area, gravity forward modeling based on the residual terrain model is only required over *k* prisms in the vicinity of the computation point (Forsberg, 1984; Hirt et al., 2010b; Wang et al., 2024). When computing derivatives of the gravitational potential such as GA and vertical deflections from the RTM, an integration radius of several tens of kilometers is generally sufficient (Hirt et al., 2010a). In this study, an integration radius of 111 km is adopted for forward modeling of the RTM-GA. To fully utilize the detailed topographic data, grid prisms with a side length of 90 m × 90 m are employed.

As shown in Fig. 5, a right-handed Cartesian coordinate system is established with the Z-axis oriented vertically downward. The gravitational disturbing potential induced at point *P* by a prism of uniform density can be formulated as:

$$T = G\rho \int_{x_1}^{x_2} \int_{y_1}^{y_2} \int_{z_1}^{z_2} \frac{1}{l} dxdydz. \tag{2}$$

The gravity disturbance can be obtained by computing the partial derivative of the disturbing potential with respect to the vertical direction, and it is given by:

$$\delta g = -\frac{\partial T}{\partial z} = G\rho \int_{x_1}^{x_2} \int_{y_1}^{y_2} \int_{z_1}^{z_2} \frac{z-c}{l^3} dxdydz . \tag{3}$$

In this formula, G denotes the gravitational constant; ρ is the density of the prism; $(x_{i,}y_{i,}z_i)$ (i=1,2) represent the coordinates of the prism's eight corners; and l is the distance from the prism's vertex to the computation point P, where $l = \sqrt{(x-a)^2 + (y-b)^2 + (z-c)^2}$.

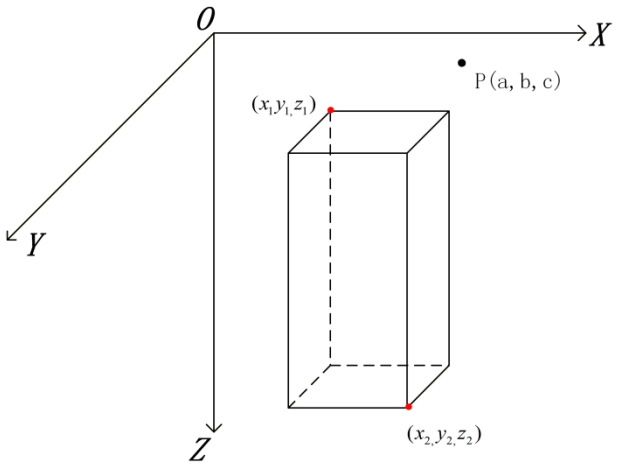

Figure 5: Prism element model.

After solving the integral, it can be expressed as:

$$\delta g(a,b,c) = -G\rho\{|||(x-a)\ln[(y-b)+l] + (y-b)\ln[(x-a)+l]$$

$$-(z-c)\arctan\frac{(x-z)(y-b)}{(z-c)l}\Big|_{x_1}^{x_2}\Big|_{y_1}^{y_2}\Big|_{z_1}^{z_2}\} . \tag{4}$$

The relationship between gravity disturbance and GA can be expressed as:

$$\Delta g = \delta g - \frac{2}{r}T . \tag{5}$$

where r denotes the geocentric radius vector of the calculation point. The gravitational contribution of an individual prism to the computation point P can be computed using the above formula, based on the spatial relationship between P and the prism's vertices. If the integration region contains a total of k prisms, the total gravity anomaly at P due to the residual terrain is obtained by summing the contributions from all individual prisms. This yields the RTM-GA Δg^{RTM}, which is expressed as:

$$\Delta g^{RTM} = \sum_{i=1}^{k} \Delta g^{RTM}(i) . \tag{6}$$

After the RTM-GA is obtained through gravity forward modeling, the XGM-GA model can be refined, and the truncation

errors can be effectively compensated. Let Δg^{XGM} denote the modeled GA before refinement. After incorporating the Δg^{RTM},

190 the refined modeled GA $\Delta g^{XGM/RTM}$ can be expressed as:

$$\Delta g^{XGM/RTM} = \Delta g^{RTM} + \Delta g^{XGM} . \quad (7)$$

Before performing the calculations, the geodetic coordinate system of the original topographic data needs to be transformed to the local Cartesian coordinate system centered on (123.5°W, 40.5°N) within the study area.

3.3 Processing of marine and coastal land areas

195 In inland areas, the computation points are located above the detailed topography. In this case, the density of the prism is set to the average crustal density, ρ_c = 2670 kg/m^3. However, over the ocean, since both the measured GA and the modeled GA are located on the sea surface, the computation points should be placed at the sea surface rather than on the detailed seafloor topography. Since the average seawater density is ρ_w = 1030 kg/m^3, the corresponding prism density should be $\Delta\rho = \rho_c - \rho_w$.

200 As shown in Fig. 6, when a terrestrial computation point is situated at the land–sea boundary, the integration region includes both land and ocean. To avoid the need to distinguish between different density values in the forward modeling process, this study adopts the RET method proposed by Hirt (2013). In the RET method, seawater is compressed into an equivalent rock mass by multiplying the ocean depth (H < 0) with a scaling factor ($1-\rho_w/\rho_c$) ≈ 0.614. With the RET method in RTM forward modeling, both the landmass and the compressed seawater mass can be assigned a uniform density

205 of ρ_c = 2670 kg/m^3, eliminating the need to differentiate the density of land and ocean prisms.

However, when using the RET method to obtain the RTM-GA at computation points in coastal land areas, the process of "compressing" seawater into an equivalent rock mass by multiplying the ocean depth (H < 0) by a coefficient factor of 0.614 causes a vertical shift in the mass center of the marine prisms. The gravitational effect of a prism at a computation point is closely related to their relative distance and position. Therefore, the displacement of prism positions caused by the

210 RET method introduces corresponding errors. Hirt (2013) also acknowledged the existence of this error and considered its effect acceptable in shallow coastal areas, hence no correction was applied. In this study, a mass center offset correction (MCOC) was applied to the marine prisms compressed by the RET method, as shown in Fig. 6.

Let H_A and H_B denote the elevations of the detailed topography and reference topography before compression, respectively. After applying the RET method, the elevations of the compressed detailed topography and reference topography are denoted

215 as H_C and H_D, respectively. After the mass center offset correction, they are represented as H_Q and H_W, with their relationships expressed as follows:

$$H_C = 0.614H_A$$
$$H_D = 0.614H_{B,} \tag{8}$$

$$H_Q = \frac{H_A + H_B}{2} + \frac{H_C - H_D}{2} = \frac{1.614H_A + 0.386H_B}{2}$$
$$H_W = \frac{H_A + H_B}{2} - \frac{H_C - H_D}{2} = \frac{0.386H_A + 1.614H_B}{2}. \tag{9}$$

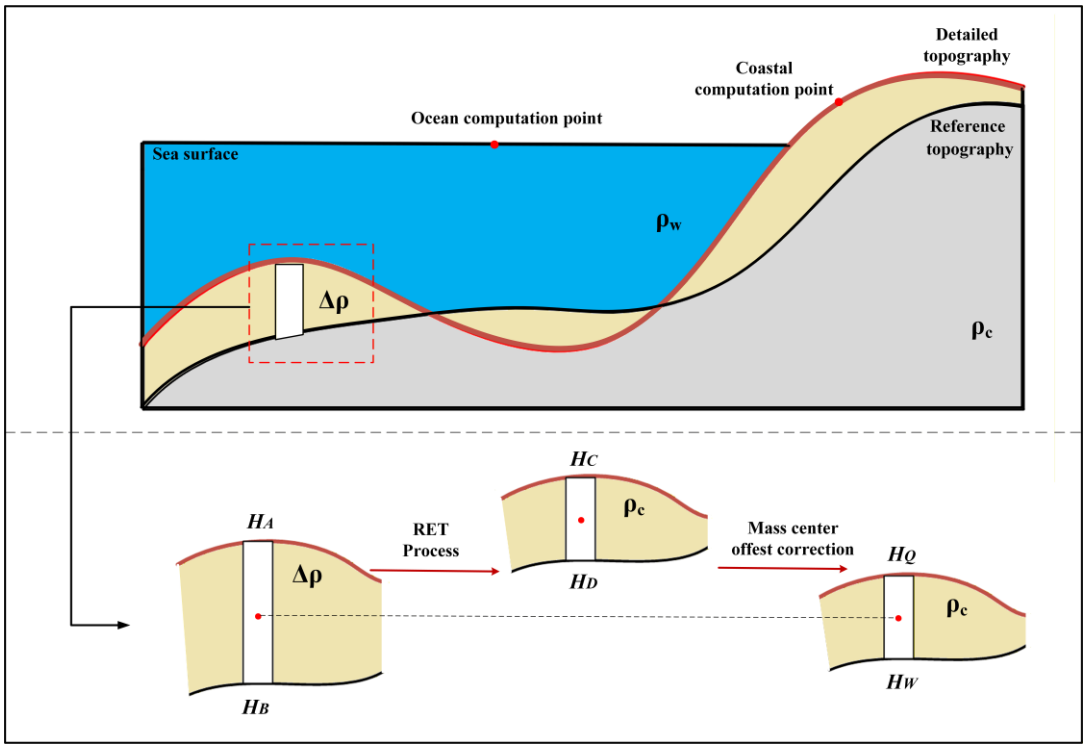

Figure 6: Location of coastal computation points and schematic diagram of the RET method and mass center offset correction.

3.4 Harmonic Correction

During the computation of the RTM-GA, a "non-harmonic" issue may arise when a computation point is located below the reference topography, as exemplified by point *P*2 in Fig. 3(a). For these points, the directly forward-modeled gravity potential is non-harmonic, necessitating a harmonic correction to satisfy the harmonic condition. This study employs the harmonic correction (HC) of the condensation method, which condenses the residual terrain mass between the computation point and the reference surface into an infinitely thin mass layer directly beneath the computation point. The purpose of this method is to transform this internal gravity field functional into a downward continued harmonic gravity field functional. This ensures that no residual mass remains above the condensed *P*2 point (Forsberg and Tscherning, 1981).

The harmonic correction formula of the condensation method can be expressed as:

$$HC = 4\pi G\rho_c \Delta h\,, \tag{10}$$

where ρ_c is the average crustal density, and $\Delta h = H^{DET} - H^{REF}$ with $\Delta h < 0$. The modeled GA corrected by RTM can be expressed as:

$$\begin{cases} \Delta g^{XGM/RTM} = \Delta g^{XGM} + \Delta g^{RTM} & \Delta h >= 0 \\ \Delta g^{XGM/RTM} = \Delta g^{XGM} + \Delta g^{RTM} + HC & \Delta h < 0. \end{cases} \tag{11}$$

Since the computation points over the ocean are located on the sea surface, harmonic correction is not required in oceanic regions.

Figure 7 presents the workflow for enhancing the XGM-GA model through the method described above.

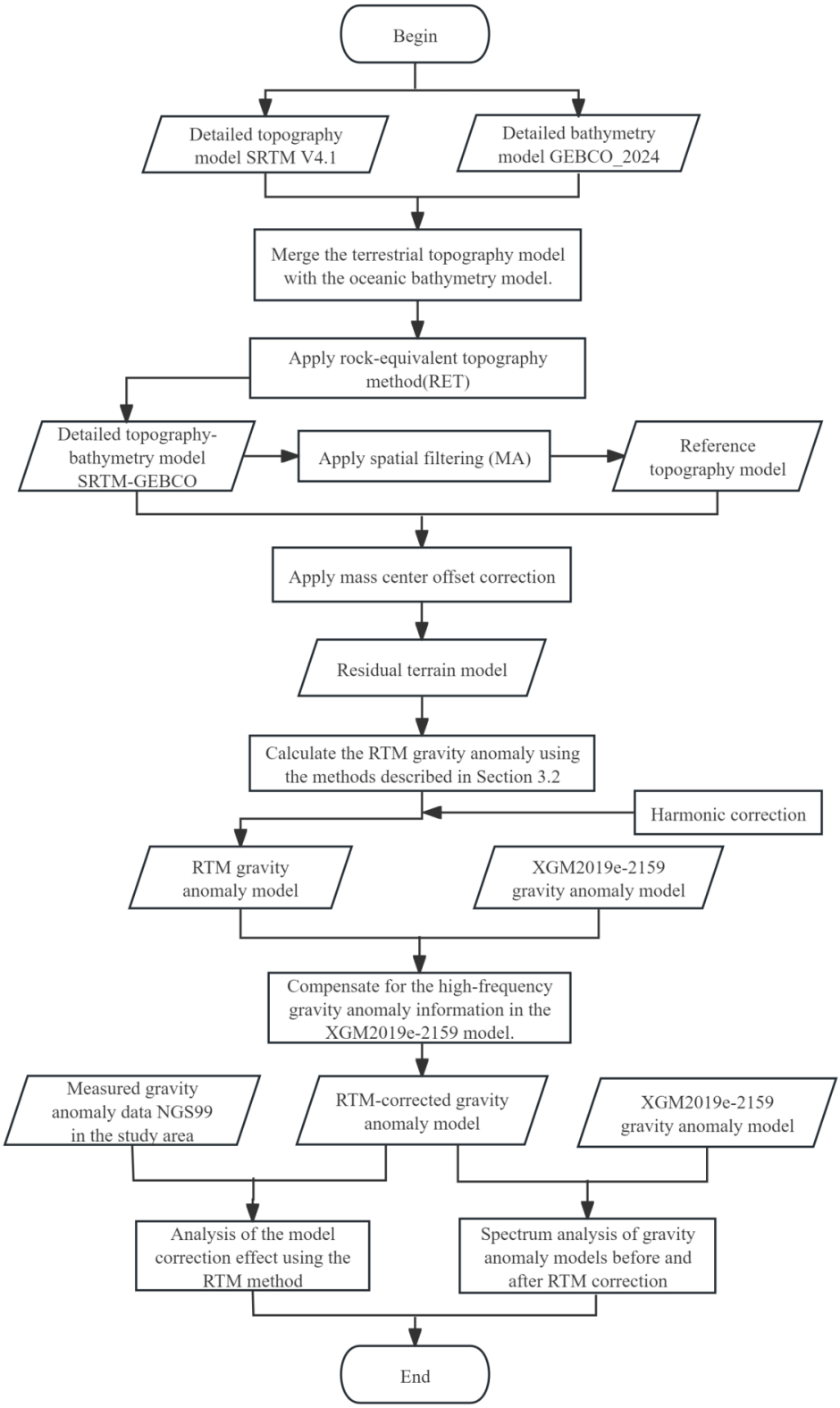

Figure 7: Workflow of XGM-GA model refinement based on RTM.

4. Experimental Results Analysis.

4.1 Computation results and overall assessment of GA

As shown in Fig. 8, the 1′×1′ RTM-GA model is computed based on the residual terrain data using Equations (2)–(6). Figure 9 shows the XGM-GA models before and after correction based on RTM gravity forward modeling. For simplicity, the RTM-corrected XGM2019e-2159 gravity anomaly model is referred to as the XGM/RTM-GA model.

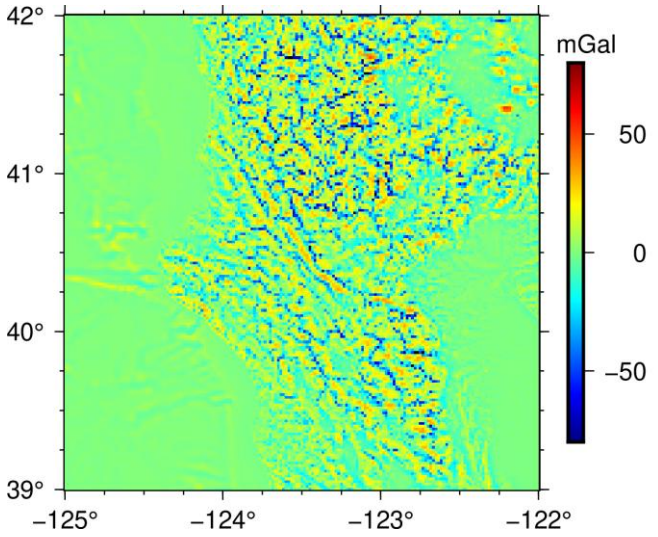

Figure 8: RTM-GA model.

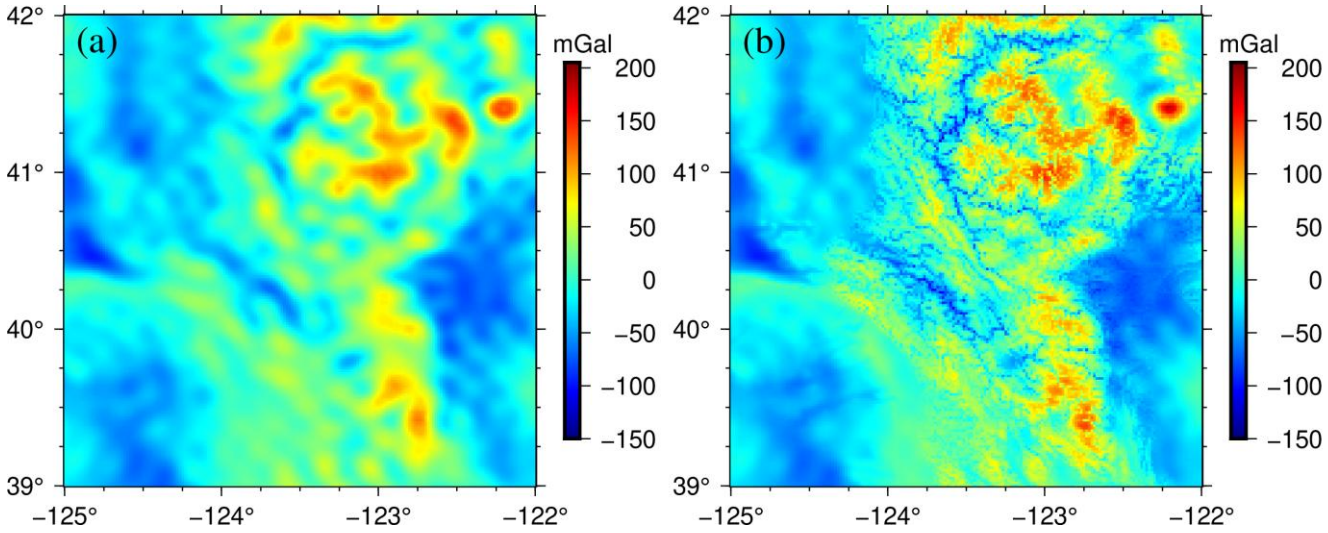

Figure 9: XGM-GA model (a) and XGM/RTM-GA model (b).

A statistical analysis of the GA from the XGM model, RTM model, and XGM/RTM model within the study area is summarized in Table 1.

Table 1: Statistical analysis of GA models (mGal)

Models	Min	Max	Mean	STD	RMS
XGM	-96.4	138.9	-2.96	39.35	39.46
RTM	-104.06	52.39	-0.70	14.70	14.71
XGM/RTM	-128.33	183.89	-3.67	42.37	42.53

Based on Figs. 8 and 9 as well as Table 1, it can be concluded that both the RMS and the standard deviation (STD) of the XGM/RTM-GA model are higher than those of the XGM-GA model. The RTM-GA model primarily reflects small-scale, high-frequency GA, which are closely associated with terrain undulations. The XGM-GA model shows a smooth spatial distribution, representing large-scale gravity variations. The XGM/RTM-GA model contains both the large-scale low-frequency information of the XGM model and the small-scale high-frequency information of the RTM model, retaining the overall trend while enhancing local details.

To verify the reliability of the results, the accuracy was evaluated using the NGS99 measured GA data. Figure 10 presents the RTM-GA computed at the locations of the measured points. By comparing Fig. 10 and Fig. 1, it can be seen that points with large absolute values of RTM-GA are mainly located in mountainous areas with significant terrain undulations, indicating that more rugged terrains contain richer high-frequency gravity signals.

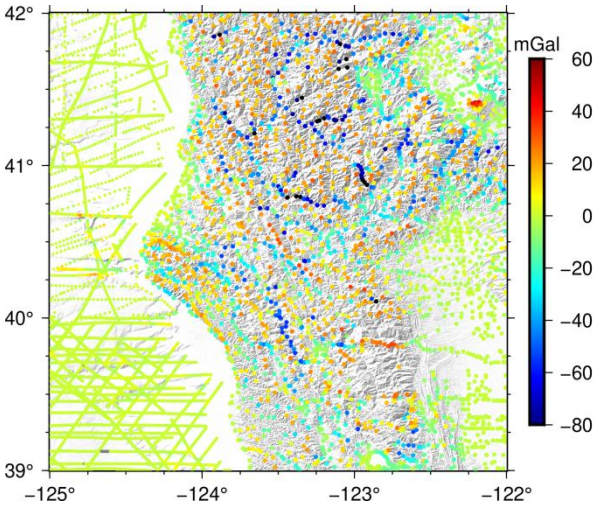

Figure 10: RTM-GA values at the measured points.

The differences between the measured GA and the XGM-GA at the measured points within the study area are calculated, as shown in Fig. 11(a). It is evident that the largest differences are concentrated in areas with rugged terrain within the study area, with the maximum absolute difference exceeding 100mGal. By adding the RTM-GA to the XGM-GA, the XGM/RTM-GA is obtained, and the difference between it and the measured GA is shown in Fig. 11(b).

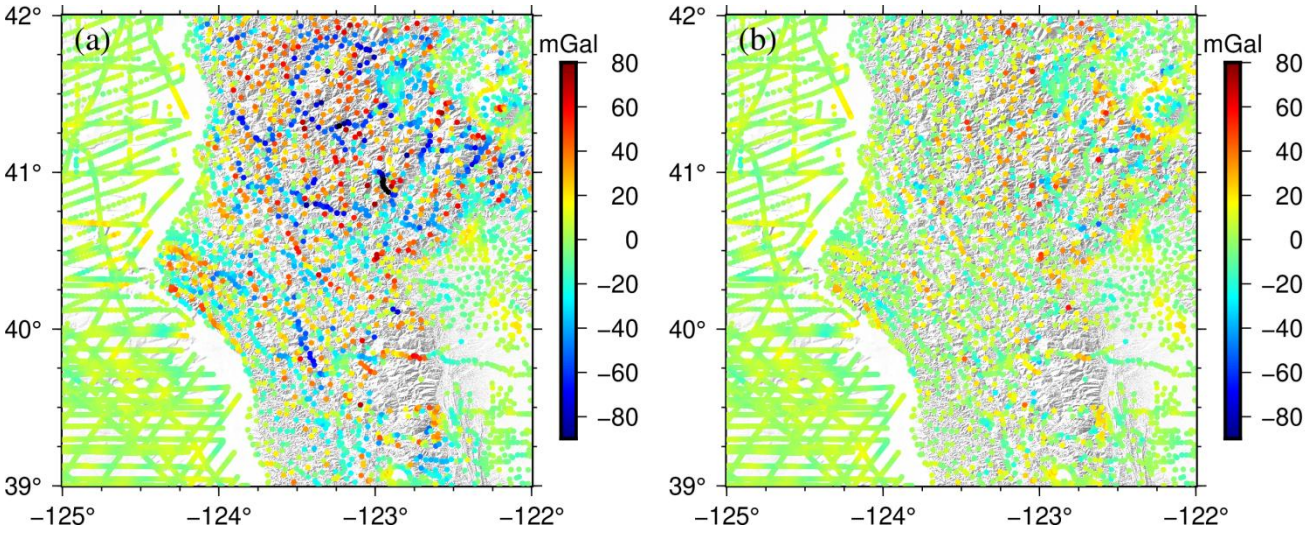

Figure 11: The difference between the measured GA and XGM-GA (a), and the difference between the measured GA and XGM/RTM-GA (b).

A comparison between Fig. 11(a) and Fig. 11(b) reveals that, following RTM correction, the difference between the modeled GA and the measured GA is significantly reduced in the central and northern regions with higher elevations, with a more uniform spatial distribution and a marked reduction in the number of high-amplitude areas. Incorporating the computed RTM-GA into the XGM-GA model can compensate for its truncation error, as the RTM-GA reflects high-frequency information that the XGM model cannot represent. The comparative statistical results between the XGM-GA and the measured GA, as well as between the XGM/RTM-GA and the measured GA at land, ocean, and all measured points, are presented in Table 2.

Table 2: Statistics of the differences between measured and modeled GA (mGal)

Point type	Variant	Min	Max	Mean	STD	RMS	IR
Land point	NGS99-XGM	-111.75	86.77	-4.66	27.67	28.06	
	NGS99-(XGM/RTM)	-51.03	60.05	1.31	13.38	13.44	52.1%
Sea point	NGS99-XGM	-19.53	24.42	2.78	5.62	6.28	
	NGS99-(XGM/RTM)	-20.81	20.46	2.44	5.30	5.83	7.1%
All point	NGS99-XGM	-111.75	86.77	1.05	14.55	14.58	
	NGS99-(XGM/RTM)	-51.30	60.05	2.18	7.95	8.25	43.4%

From Table 2, it can be seen that the accuracy of the GA model is improved on both land and sea after applying the RTM correction. At the land measurement points, the RMS of the difference between the measured GA and the XGM-GA decreased by 14.62mGal, with an improvement rate (IR) of 52.1%. At the ocean measurement points, the RMS of the difference decreased by 0.45mGal, with an IR of 7.1%. Overall, at all measurement points, the RMS of the difference decreased by 6.33mGal, with an IR of 43.4%. According to the statistics, the accuracy of the XGM-GA model is lower in land areas and higher in ocean regions, while the RTM correction is significantly more effective in land areas than in ocean regions.

To investigate the correction effect of the RTM method at different elevations, the measured GA points were classified into five categories based on elevation. The elevation ranges for these five categories are [-3400m, -1600m), [-1600m, 0m), [0m, 500m), [500m, 1500m), and [1500m, 4000m), with 5035, 5762, 1498, 1360, and 389 points, respectively. The RTM-GA was calculated separately for these five categories of points, and the XGM-GA and XGM/RTM-GA were compared with the measured GA for each category. The statistical results are shown in Table 3.

Table 3: Statistics of the differences between measured and modeled GA at different elevations (mGal)

Elevation Range	Point Numbers	Variant	Min	Max	Mean	STD	RMS
[-3400m, -1600m)	5035	NGS99-XGM	-19.53	18.05	2.47	4.37	5.02
		NGS99(XGM/RTM)	-20.69	13.89	2.34	4.21	4.82
[-1600m, 0m)	5762	NGS99-XGM	-18.68	24.42	3.05	6.51	7.18
		NGS99(XGM/RTM)	-20.81	20.46	2.53	6.09	6.60
[0m, 500m)	1498	NGS99-XGM	-87.52	29.45	-12.63	20.16	23.79
		NGS99(XGM/RTM)	-36.26	36.80	-0.32	9.39	9.40
[500m, 1500m)	1360	NGS99-XGM	-111.75	61.17	-3.76	29.00	29.24
		NGS99(XGM/RTM)	-51.30	55.03	0.69	13.98	13.99
[1500m, 4000m)	389	NGS99-XGM	-75.85	86.77	22.83	29.93	37.65
		NGS99(XGM/RTM)	-46.36	60.05	9.80	19.74	22.04

From the table above, it can be seen that the higher the elevation on land, the greater the difference between the modeled and measured values; the deeper the ocean, the smaller the difference at the sea surface between the modeled and measured values. This suggests that areas with greater terrain undulation on land have lower modeled GA accuracy, as the terrain contributes to the omission of high-frequency information in the modeled GA. At sea surface measurement points, the shallower the water, the closer the seafloor terrain is to the measurement point. Consequently, the gravitational effect produced by the residual seafloor topography at these points is greater, leading to better correction results with the RTM method. The RMS values at these five types of points were reduced by 0.20mGal, 0.58mGal, 14.39mGal, 15.25mGal, and 15.61 mGal, respectively. It is evident that as the elevation increases, the RTM correction effect also increases.

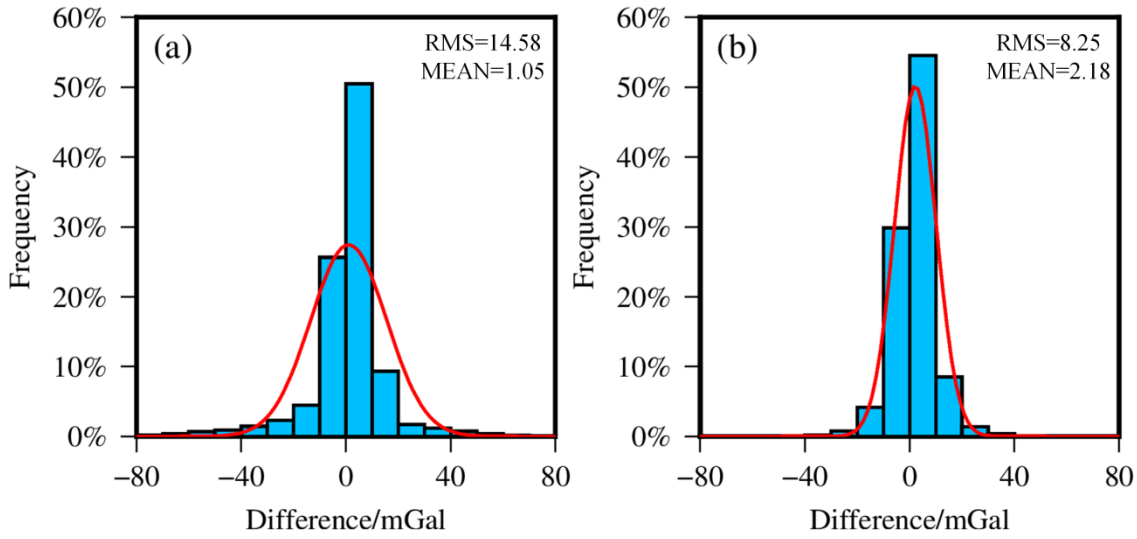

Figure 12: Histogram of the differences between the measured GA and XGM-GA (a), and the differences between the measured GA and XGM/RTM-GA (b).

Figure 12 shows the distribution histograms of the differences between the measured GA and both the XGM-GA and

XGM/RTM-GA at all measured points in the study area. Statistical analysis shows that 93.75% of the differences between the measured GA and XGM-GA fall within ±30mGal, while this proportion increases to 99.15% for the differences between the measured GA and XGM/RTM-GA. These findings demonstrate a notable improvement in data quality resulting from the application of the RTM method.

4.2 Gravity Anomaly Assessment in Coastal Land Areas

When a terrestrial computation point is located in a coastal area, the integration region includes both land and ocean. The standard calculation requires distinguishing rectangular prisms with different densities for land and ocean, which reduces computational efficiency and increases the computational burden. To avoid the need to distinguish between different density values during the forward modeling process, this study employs the RET method, compressing seawater into an equivalent rock mass while incorporating mass center offset correction.

A 6-km landward buffer zone was established along the coastline to identify measured points where the integration region includes both land and ocean. In the study area, 264 land-coastal points were selected for forward modeling of RTM-GA using the RET method. The calculations considered three cases: residual terrain in the land region, residual terrain in the ocean region, and residual terrain in the entire integration region. The statistical results are presented in Table 4.

Table 4: GA statistics at land-coastal points (mGal)

Variant	RTM	Min	Max	Mean	STD	RMS	IR
NGS99-XGM	Not applied	-32.62	49.71	0.75	14.96	14.98	
NGS99-(XGM/RTM)	Land-only	-19.51	30.02	1.98	8.48	8.71	41.8%
	Sea-only (without-MCOC)	-29.08	47.02	0.35	14.63	14.64	2.3%
	Sea-only (with-MCOC)	-26.54	49.82	3.01	13.95	14.27	4.7%
	Land/sea (without-MCOC)	-23.52	28.11	2.08	7.95	8.22	45.1%
	Land/sea (with-MCOC)	-18.54	28.61	1.79	7.77	7.97	46.8%

The statistical results indicate that using residual terrain on both land and ocean can refine the XGM-GA to varying degrees. Compared to the measured GA, the RMS difference is reduced by 6.27mGal when considering only residual terrain on land (setting RTM elevation over the ocean to zero). When considering only residual terrain in the ocean (setting RTM elevation over land to zero), the RMS reduction is 0.71mGal. When considering all residual terrain, the RMS difference is reduced by 7.01mGal.

It is noteworthy that when only the ocean residual terrain is considered, the RMS is reduced by only 0.34mGal without applying the MCOC, whereas it decreases by 0.71mGal when the correction is applied. When both marine and terrestrial residual terrain are considered, the application of the MCOC further reduces the RMS by 0.25mGal compared to the case without applying it. This indicates that introducing the mass center offset correction in the RET method can effectively enhance the accuracy of the model.

4.3 Power Spectral Density Analysis

To more comprehensively reflect the effects of RTM correction on the XGM-GA, a power spectral density (PSD) analysis was conducted in the frequency domain for both the XGM-GA model and the XGM/RTM-GA model. The results are shown in Fig. 13. PSD analysis is a commonly used method for evaluating signal characteristics in the frequency domain, which effectively reveals the energy distribution of data across different frequencies. At the same wavelength, a higher PSD value indicates that the model contains greater energy and more complete information.

According to statistical analysis, the PSD of the XGM-GA and XGM/RTM-GA models are nearly identical in the medium-to-long-wavelength range, where wavelengths exceed 39.5 km. In the wavelength range of 18.7 km to 39.5 km, the PSD of the XGM/RTM model exhibits a slight increase compared to that of the XGM model. For wavelengths shorter than 18.7 km, the PSD of the XGM/RTM model shows a substantial enhancement relative to the XGM model. These results indicate that the XGM-GA model contains more high-frequency information, confirming that the RTM method effectively compensates for the deficiency of high-frequency components in the model and reduces its truncation error.

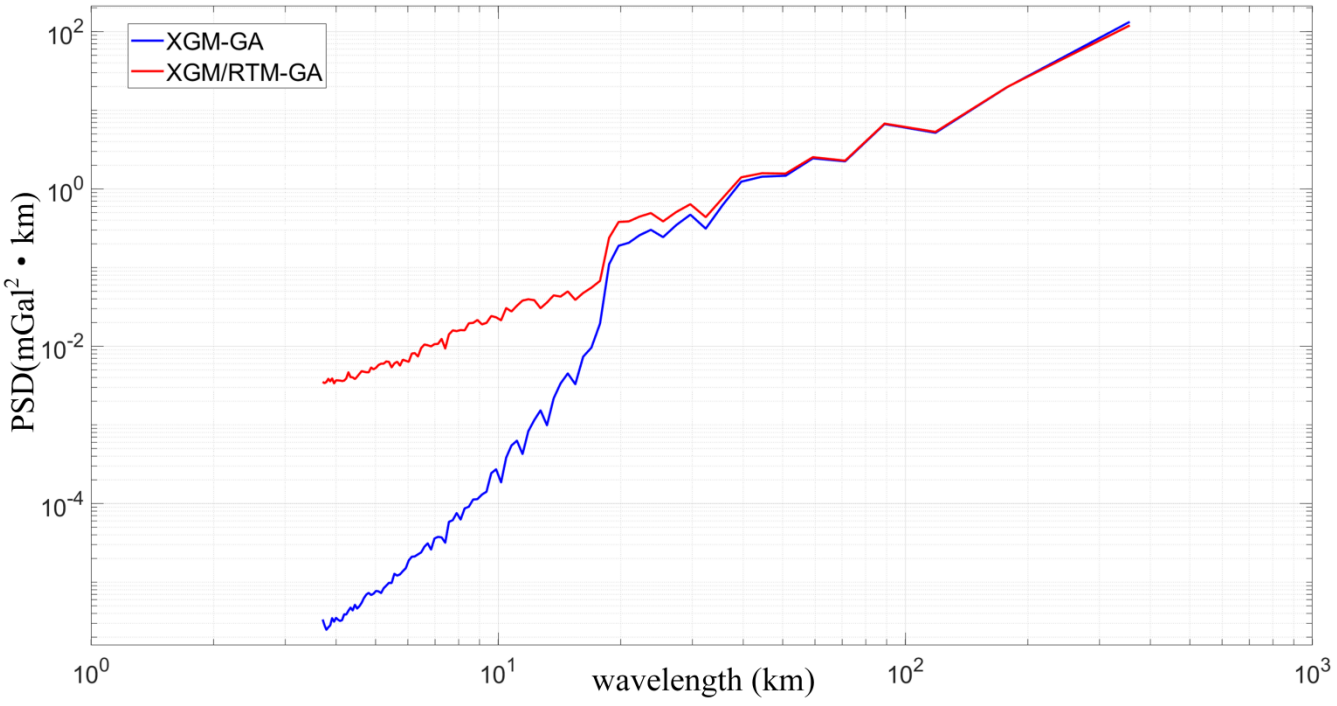

Figure 13: PSD of the XGM-GA and XGM/RTM-GA models.

5. Conclusions and Outlook

In this study, the XGM-GA model in coastal areas was refined by constructing residual terrain using detailed topographic and bathymetric data. Gravity forward modeling based on the RTM spatial domain method was employed to effectively compensate for the missing high-frequency components in the XGM2019e-2159 model. To ensure computational efficiency and accuracy, the RET method and mass center offset correction were applied in constructing the residual terrain model for coastal areas. Consequently, the XGM/RTM-GA model was obtained for the study area. Finally, the accuracy of the XGM/RTM-GA model was validated using measured GA data from NGS99. The results show that the XGM-GA in coastal areas was significantly improved after RTM correction, with high-frequency signals effectively extended.

Statistical calculations show that after RTM correction, the XGM-GA model's precision improved by 6.33mGal, with an IR of 43.4%. Overall, it is much more consistent with the measured values, and the quality of the model has significantly improved. With increasing elevation, the accuracy of the XGM-GA declines, while the magnitude of the RTM correction becomes more significant. This also confirms that terrain is an important source of high-frequency signals in GA models. At coastal land points, the gravity forward modeling of both marine residual topography and terrestrial residual topography can improve the accuracy of the XGM-GA to varying extents. Finally, by analyzing the PSD of the XGM-GA and XGM/RTM-GA models, it can be seen that the RTM correction effectively compensates for the missing high-frequency signals in the GA model.

Therefore, in the future, the method presented here for computing gravity in coastal areas could be applied to the construction of high-resolution coastal gravity field models, while integrating existing high-resolution gravity field models over land. This represents a promising direction for further research. Finally, it should be noted that the NGS99 measured data, released in 1999, are only distributed over the U.S. mainland and its adjacent coastal regions. Therefore, in future work, updated measured data should be used according to the study area, especially over marine regions, where the quality and quantity of shipborne gravity data have significantly improved. For subsequent refinements of gravity field models in oceanic areas, it is recommended to consider using newly released shipborne gravity data in combination with satellite altimetry-derived ocean gravity data.

Code availability

All data used in this study are publicly available through the XGM-GA (http://icgem.gfz-potsdam.de/calcgrid), GEBCO (https://www.gebco.net), SRTM (https://srtm.csi.cgiar.org), and NGS99(https://www.ncei.noaa.gov/products/gravity-data). The source code and gravity anomaly model data before and after improvement are available at: https://doi.org/10.5281/zenodo.15300546

Author contributions

Conceptualization: YL, JG. Methodology: YL, JG. Validation: YL, JG, BG, SB, HS, XL. Writing – original draft: YL.

Writing – review & editing: YL, JG, BG, SB, HS, XL. All authors contributed to writing and revising the manuscript.

Competing interests

The contact author has declared that none of the authors has any competing interests.

Acknowledgements

We express our gratitude to the following organizations: the National Aeronautics and Space Administration (NASA) and the National Imagery and Mapping Agency (NIMA) for providing the SRTM V4.1 digital elevation model, the International Hydrographic Organization (IHO) and the Intergovernmental Oceanographic Commission of UNESCO (IOC) for providing the GEBCO_2024 bathymetric data, the National Geospatial-Intelligence Agency (NGA) for supplying the XGM2019e-2159 gravity field model, and the National Geodetic Survey (NGS) for offering the measured gravity anomaly data.

Financial support

This research has been supported by the National Natural Science Foundation of China (grant Nos. 42430101, 42274006, and 42192535).

References

Andersen, O. B., Knudsen, P., and Berry, P. A.: The DNSC08GRA global marine gravity field from double retracked satellite altimetry, Journal of Geodesy., 84, 191–199, doi: 10.1007/s00190-009-0355-9, 2010.

Claessens, S. J.: Evaluation of gravity and altimetry data in Australian coastal regions, in: Geodesy for Planet Earth: Proceedings of the 2009 IAG Symposium, Buenos Aires, Argentina, 31 August – 4 September 2009, edited by: Kenyon, S., Pacino, M., and Marti, U., Springer, Berlin, 435–442, 2011.

Dubey, C. P. and Roy, A.: Joint inversion of gravity and gravity gradient and its application to mineral exploration, J. Ind. Geophys. Union, 27, 1–18, 2023.

Forsberg, R.: A study of terrain reductions, density anomalies and geophysical inversion methods in gravity field modelling, Report 355, Department of Geodetic Science and Surveying, Ohio State University, Columbus, 1984.

Forsberg, R. and Tscherning, C. C.: The use of height data in gravity field approximation by collocation, J. Geophys. Res., 86, 7843–7854, doi: 10.1029/JB086iB09p07843, 1981.

Gruber, T.: Evaluation of the EGM2008 gravity field by means of GPS-levelling and sea surface topography solutions, Technical Report, Institut für Astronomische und Physikalische Geodäsie, Munich, 2009.

Guo, J., Gao, Y., Hwang, C., and Sun, J.: A multi-subwaveform parametric retracker of the radar satellite altimetric waveform and recovery of gravity anomalies over coastal oceans, Sci. China Earth Sci., 53, 610–616, doi: 10.1007/s11430-009-0171-3 2010.

Han, S. C., Sauber, J., and Pollitz, F.: Coseismic compression/dilatation and viscoelastic uplift/subsidence following the 2012 Indian Ocean earthquakes quantified from satellite gravity observations, Geophysical Research Letters., 42, 3764–3772, doi:10.1002/2015GL063819, 2015.

Hirt, C.: Prediction of vertical deflections from high-degree spherical harmonic synthesis and residual terrain model data, Journal of Geodesy, 84, 179–190, doi: 10.1007/s00190-009-0354-x, 2010.

Hirt, C.: RTM gravity forward-modeling using topography/bathymetry data to improve high-degree global geopotential models in the coastal zone, Marine Geodesy., 36, 183–202, doi: 10.1080/01490419.2013.779334, 2013.

Hirt, C., Featherstone, W. E., and Marti, U.: Combining EGM2008 and SRTM/DTM2006.0 residual terrain model data to improve quasigeoid computations in mountainous areas devoid of gravity data, Journal of Geodesy, 84, 557–567, doi: 10.1007/s00190-010-0359-1, 2010a.

Hirt, C., Marti, U., Bürki, B., and Featherstone, W. E.: Assessment of EGM2008 in Europe using accurate astrogeodetic vertical deflections and omission error estimates from SRTM/DTM2006.0 residual terrain model data, Journal of Geophysical Research., 115, B10404, doi: 10.1029/2009JB007057, 2010b.

Hwang, C.: Analysis of some systematic errors affecting altimeter-derived sea surface gradient with application to geoid determination over Taiwan, Journal of Geodesy., 71, 113–130, doi: 10.1007/s001900050080, 1997.

Ince, E. S., Abrykosov, O., Förste, C., and Flechtner, F.: Forward gravity modelling to augment high-resolution combined gravity field models, Surv. Geophys., 41, 767–804, doi: 10.1007/s10712-020-09590-9, 2020.

Ke, B., Zhang, L., Xu, J., Zhang, C., and Dang, Y.: Determination of the mean dynamic ocean topography model through combining multi-source gravity data and DTU15 MSS around China's coast, Advances in Space Research., 63(1), 203–212, doi: 10.1016/j.asr.2018.10.040, 2019.

Kuhn, M. and Hirt, C.: Topographic gravitational potential up to second-order derivatives: an examination of approximation errors caused by rock-equivalent topography (RET), Journal of Geodesy., 90, 883–902, doi:10.1007/s00190-016-0917-6, 2016.

Li, X., Lin, M., Krcmaric, J., and Carignan, K.: Bathymetric effect on geoid modeling over the Great Lakes area, Earth, Planets and Space., 76, 14, doi: 10.1186/s40623-024-01961-5, 2024.

Li, Z., Guo, J., Zhu, C., Liu, X., Hwang, C., Lebedev, S., Chang, X., Soloviev, A., and Sun, H.: The SDUST2022GRA global marine gravity anomalies recovered from radar and laser altimeter data: contribution of ICESat-2 laser altimetry, Earth System Science Data., 16, 4119–4135, doi: 10.5194/essd-16-4119-2024, 2024.

Liang, S., Wang, X., Xu, Z., Dai, Y., Wang, Y., Guo, J., Jiao, Y., and Li, F.: Steep subduction of the Indian continental mantle lithosphere beneath the eastern Himalaya revealed by gravity anomalies, Sci. China Earth Sci., 66(9), 1994–2010, doi: 10.1007/s11430-022-1110-y, 2023.

Lin, M., Yang, M., and Zhu, J.: Experiences with the RTM method in local quasi-geoid modeling, Remote Sensing., 15, 3594, doi: 10.3390/rs15143594, 2023.

Liu, Y., Guo, J., Lin, M., Chang, L., Chang, X., and Liu, X.: Refining regional gravity anomalies and vertical deflections of high-degree earth gravity model from residual terrains based on the spatial domain method, Earth, Planets and Space., 77, 37, doi: 10.1186/s40623-025-02168-y, 2025.

Parker, R. L.: Improved Fourier terrain correction. Part I, Geophysics., 60, 1007–1017, doi:10.1190/1.1443829, 1995.

Pavlis, N. K., Holmes, S. A., Kenyon, S. C., and Factor, J. K.: The development and evaluation of the Earth Gravitational Model 2008 (EGM2008), Journal of Geophysical Research: Solid Earth, 117, B04406, doi: 10.1029/2011JB008916, 2012.

Reuter, H. I., Nelson, A., and Jarvis, A.: An evaluation of void-filling interpolation methods for SRTM data, International Journal of Geographical Information Science., 21, 983–1008, doi:10.1080/13658810601169899, 2007.

Smith, D. A.: The gravitational attraction of any polygonally shaped vertical prism with inclined top and bottom faces, Journal of Geodesy., 74, 414–420, doi: 10.1007/s001900000102, 2000.

Tenzer, R.: Spectral domain of Newton's integral, Bollettino di Geodesia e Scienze Affini., 64, 61–73, 2005.

Tozer, B., Sandwell, D. T., Smith, W. H., Olson, C., Beale, J. R., and Wessel, P.: Global bathymetry and topography at 15 arc sec: SRTM15+, Earth and Space Science., 6, 1847–1864, doi: 10.1029/2019EA000658, 2019.

Tsoulis, D., Novák, P., and Kadlec, M.: Evaluation of precise terrain effects using high-resolution digital elevation models, Journal of Geophysical Research: Solid Earth., 114, B02404, doi: 10.1029/2008JB005639, 2009.

Wang, L., Yang, M., Huang, Z., Feng, W., Yan, X., and Zhong, M.: Impacts of digital elevation model elevation error on terrain gravity field calculations: a case study in the Wudalianchi airborne gravity gradiometer test site, China, Remote Sensing., 16, 3948, doi: 10.3390/rs16213948, 2024.

Wild-Pfeiffer, F.: A comparison of different mass elements for use in gravity gradiometry, Journal of Geodesy., 82, 637–653, doi: 10.1007/s00190-008-0219-8., 2008.

Wu, L. and Chen, L.: Fast computation of terrain-induced gravitational and magnetic effects on arbitrary undulating surfaces, Surveys in Geophysics., 44, 1175–1210, doi: 10.1007/s10712-023-09773-0, 2023.

Yang, M., Hirt, C., Rexer, M., Pail, R., and Yamazaki, D.: The tree-canopy effect in gravity forward modelling, Geophysical Journal International., 219, 271–289, doi: 10.1093/gji/ggz264, 2019.

Zhou, R., Guo, J., Ya, S., Sun, H., and Liu, X.: SDUST2023VGGA: a global ocean vertical gradient of gravity anomaly model determined from multidirectional data from mean sea surface, Earth System Science Data., 17, 817–836, doi: doi.org/10.5194/essd-17-817-2025, 2025.

Zingerle, P., Pail, R., Gruber, T., and Oikonomidou, X.: The combined global gravity field model XGM2019e, Journal of Geodesy, 94, 66, doi: 10.1007/s00190-020-01398-0, 2020.